Chapter 1

Introduction

1.1 Motivation

Turbulence remained as “the last great unsolved problem in classical physics”, a description attributed to Feynman, Heisenberg and many great scientific minds. For almost a century, wall bounded turbulent shear flows have been regarded as an attractive topic for physicists, mathematicians and engineers and has inspired wide ranges of studies. In most practical and industrial applications, the Reynolds number acquires very high values. Therefore, detailed study of this phenomenon at high Reynolds numbers is of fundamental importance for a realistic prediction of losses, efficient flow control and reduction of energy consumption.

The present research focuses on fully developed turbulent pipe flow at high Reynolds numbers as one of the canonical forms of wall turbulence. This geometry provides homogenous turbulence in streamwise and azimuthal directions as well as the possibility for more accurate determination of wall shear stress. In flows at high Reynolds numbers, an appreciable length of logarithmic behavior is observable in the mean velocity and streamwise turbulence intensity profiles. In such cases, the logarithmic region contributes most to the bulk turbulence production as observable in Figure 1.1, where the area below the premultiplied profiles, represents the overall energy production (Smits, McKeon, and Marusic (2010)). Furthermore, as highlighted in Figure 1.2, in such regimes energy containing structures with lower wavenumbers are clearly distinguished from the small scale structures in the dissipation range. Therefore, the existence of a wider overlap layer and sufficient separation between the scales at highly turbulent regimes provides for a clearer and more distinguished observation of structures with different length scales.

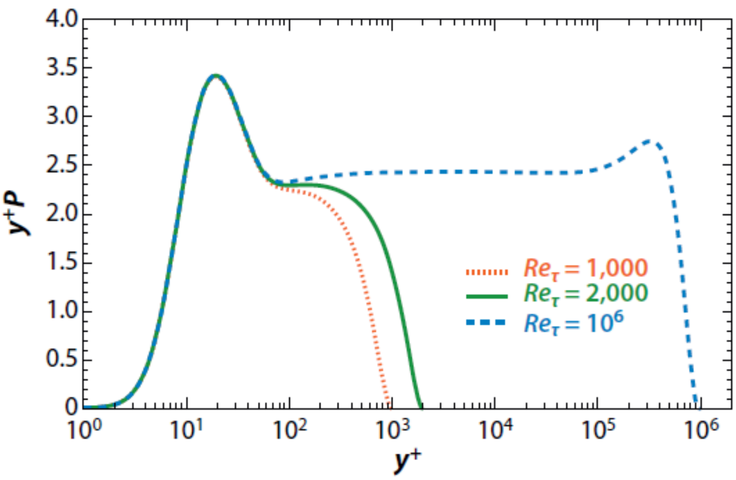

FIGURE 1.1: Turbulent kinetic energy production at $y^+ \approx 12$ for various Reynolds numbers. (Smits, McKeon, and Marusic (2010))

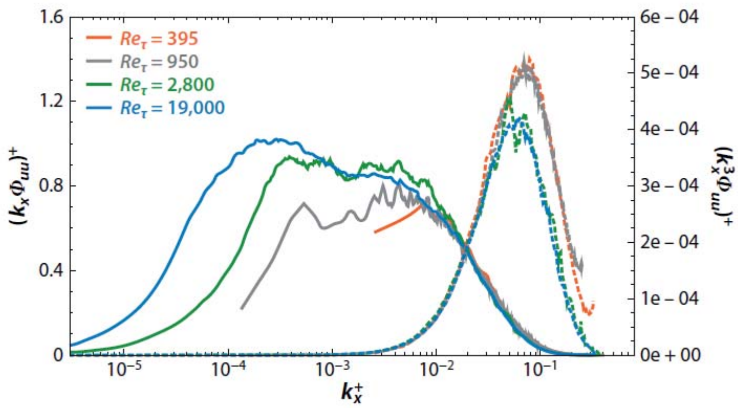

FIGURE 1.2: Streamwise velocity spectra at $y^+ \approx 12$ for various Reynolds numbers. (Smits, McKeon, and Marusic (2010))

In the past decades three different areas of focus have emerged: structures and scaling of turbulence; observation and identification of turbulent coherent structures and more recently large- and very large-scale motions (LSM and VLSM):

- Almost since the beginning of wall turbulence investigations in the 1950's, one important focus of research has been on the structure and scaling of turbulence. Some of the most prominent observations were done by Coles (1956), Patel and Head (1969a), Perry and Abell (1975), Barenblatt (1993a), Barenblatt (1993b), Eggels et al. (1994), Zagarola and Smits (1998), McKeon et al. (2004a), McKeon et al. (2004b) and Morrison et al. (2004).

- In the 1970's a second group of wall bounded turbulence studies were inspired by observation of coherent structures. Better understanding of such structures was of interest for a large number of researchers like Townsend (1961) and more recently Hutchins and Marusic (2007), Bailey et al. (2008), Monty et al. (2007) and Monty et al. (2009). They resulted in vital information about flow dynamics and provided good inputs to flow control methodologies. Furthermore, the interactions between flow structures and scaling properties of wall-bounded shear flows has been the subject of major studies including those of Monty et al. (2007) and Monty et al. (2009).
- During the recent years new observations have been addressed by Kim and Adrian (1999), Morrison et al. (2004) and Vallikivi, Ganapathisubramani, and Smits (2015) concerning the existence of very large-scale motions (VLSM).

Numerical study of fully developed turbulent pipe flow has been treated since the first simulations by Eggels et al. (1994). In spite of the increased interest in DNS of this type of flow, the simulations are still limited in Reynolds numbers and domain size. Recent studies like Feldmann and Wagner (2012) and El Khoury et al. (2013) have extended the bulk Reynolds number limits to $Re_b \approx 40.000$ focusing on the statistical flow properties. Turbulent coherent structures and their interactions have been the target of many studies like Wagner and Friedrich (1998), Wu, Baltzer, and Adrian (2012) and Schlatter et al. (2014). Effects of compressibility on statistics of pipe flow have been studied by Ghosh, Sesterhenn, and Friedrich (2006). An alternative approach to study coherent motions is to directly solve for exact solutions of the Navier-Stokes equations. Relative periodic orbits embedded in turbulence have been obtained in pipe flow by Avila et al. (2013) and Willis, Cvitanoic, and Avila (2013). However, this has so far been tested in transitional flows.

One of the recent focuses of wall bounded turbulence studies has been concentrated on scaling and analysis of turbulence intensity profiles which represent diagonal components of Reynolds stress tensor. Measurements of Morrison et al. (2004) and more recently Hultmark, Bailey, and Smits (2010) in the Superpipe in Princeton revealed the existence of an inner peak in the mentioned profile at where turbulent kinetic energy production reaches its maximum as well. These observations have convincingly proven that this inner peak does not reflect a strong dependence on Reynolds number in pipe flow as shown in Figure 1.3 (where u_τ corresponds to shear Reynolds number based on radius and friction velocity). This is contrary to boundary layer flow where the inner peak grows with increasing Reynolds number indicating a growing outer layer influence on the near wall motions. The reason for invariance of the inner peak in pipe flow is still not fully understood. However, considering that the velocity spectra show Reynolds number variation, one possible explanation is that interactions between scales continue evolving while the overall energy is kept constrained by streamwise homogeneity in pipe flow (Smits, McKeon, and Marusic (2010)). The same experimental data have shown emergence of a second peak or plateau at higher Reynolds numbers. As proposed by Morrison et al. (2004) this so called outer peak taking place in the overlap layer may represent structural changes that can show presence of new outer phenomena. Nevertheless, such behavior has not been considered in any formulations for streamwise turbulence intensity so far (Smits, McKeon, and Marusic (2010)).

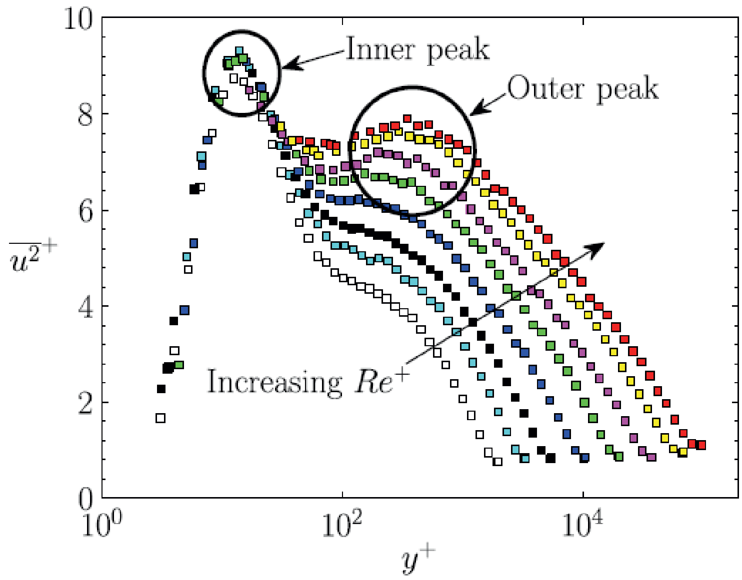

FIGURE 1.3: Inner scaled turbulence fluctuations for $2.000 \leq Re^+ \leq 100.000$ in Superpipe. (Hultmark et al. (2012))

1.2 Large-Scale Structures in Wall-Bounded Turbulence

The character of wall-bounded turbulence with increasing Reynolds number remains a particular phenomena which reflects its importance to recent studies in canonical turbulent flows (boundary layer, pipe, channel). A specific question is the length of the so-called large- and very large-scale motions (LSM & VLSM) in the outer layer of fully developed turbulent pipe flow in terms of their turbulence spectrum at various Reynolds numbers. The inertia of turbulent motions is dominated far from the wall since the viscosity is highly affected in the near-wall regions. The flow is dictated by the scales influenced by viscosity which are labeled as inner scales whereas the outer scales are effective far from the wall.

In canonical geometries the apparent shear layer scale is considered in flat plate boundary layers as δ, the boundary layer thickness, in pipe as R, the pipe radius and in channel as h, the half-width of the channel. The consistent velocity in the region closest to the wall is the friction velocity $u_\tau = \sqrt{\tau_w/\rho}$, where τ_w is the wall shear stress and ρ the density of the fluid. The viscous length scale is defined as $l^* = \nu/u_\tau$ which can also be interpreted as $l^* = R/Re_\tau$, where ν stands for kinematic viscosity and Re_τ for friction Reynolds number which can be determined as $Re_\tau = u_\tau R/\nu$ for pipe flow. The ratio of the inner and outer scales is R^+ called the Kármán number or friction Reynolds number. A large divergence between these length scales observed at high Reynolds numbers which delivers an additional region, the turbulent wall region $\nu/u_\tau \leq y \leq R$. This region is divided by three different scale ranges in terms of the turbulence spectrum (Perry, Henbest, and Chong (1986)): high wavenumber range corresponds to motions with the Kolmogorov length scale η_K; intermediate wavenumbers with wall-normal scale y and low wavenumbers with R. Spectral characteristics of turbulence have illuminated the relevance of large-scale motions in the form of long regions of streamwise velocity fluctuations in the outer layer. Their energetically existence has been first recognized in turbulent boundary layer by observing a long tail on the temporal auto-correlation of streamwise velocity (Townsend (1958),Grant (1958)). They are also identified by detecting a major peak in the spectrum of instantaneous streamwise velocity component (premultiplied one-dimensional spectra as function of distance from the wall, Figure 1.6) at various wavenumbers (Grant (1958),Kim and Adrian (1999)). These motions contain half of the turbulent kinetic energy of the streamwise velocity component and more than half of the Reynolds shear stress (Kim and Adrian (1999),Bullock, Cooper, and Abernathy (1978)).

There are number of existing hypothesis about the length of the energetic motions and no commonly accepted definition of LSMs and VLSMs. The

LSMs or turbulent bulges have usually been described as an argument of long correlation tails related to the "large-eddy hypothesis" proposed by Bullock, Cooper, and Abernathy (1978), but nevertheless recent studies provide a wider overview about their interpretation. Kim and Adrian (1999) suggested with their single-point hot-wire measurements in pipe flow that these motions with wavelengths of approximately $2R$-$3R$ should be linked to the streamwise alignment of hairpin vortices into hairpin packets and structures longer than $14R$ can be characterized as VLSM (Figure 1.4 and Figure 1.5). According to same study, VLSMs are prominent within the logarithmic layer and their evidence is depending on power spectrum of the streamwise velocity fluctuations based on Taylor's hypothesis of frozen turbulence. Pre-multiplied power spectra is used to indicate the peaks of turbulent motions which was also preferred by Perry and Abell (1975) for revealing the bi-modal distribution of wavelengths. Bullock, Cooper, and Abernathy (1978) reported that these structures should be referred as LSM if their lengths in streamwise direction are between $0.1\pi\mathrm{R}{-}\pi\mathrm{R}$ and structures larger than $(\approx 3R)$ should be considered as VLSM. To distinguish LSM and VLSM wavenumber ranges the wavenumber $k_x R = 2$ is taken as boundary. It corresponds to a wavelength of $\pi\mathrm{R}$ $(\approx 3R)$ which is approximately the size of the accepted mean bulge and at $y/R = 0.5$ the longest streamwise wavelength λ_{max} is detected as $\approx 20R$. Here k_x is the streamwise wavenumber and $k_x R$ is the non-dimensional wavenumber. k_x is derived from Taylor's hypotesis, so that k_x=$2\pi\mathrm{f}/U$ and λ_x is determined using the same relation as $k_x = 2\pi/\lambda_x$. The same procedure with dividing line between LSM and VLSM at $k_x R$=2 is also used by Balakumar and Adrian (2007).

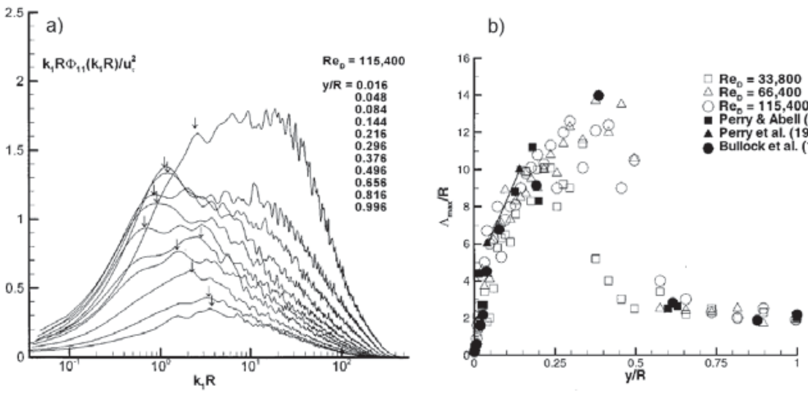

FIGURE 1.4: a) Premultiplied spectra as functions of distance from the wall; b) the dimensionless wavelength of the very large-scale motion correlates with other experiments in pipe flow. (Kim and Adrian (1999))

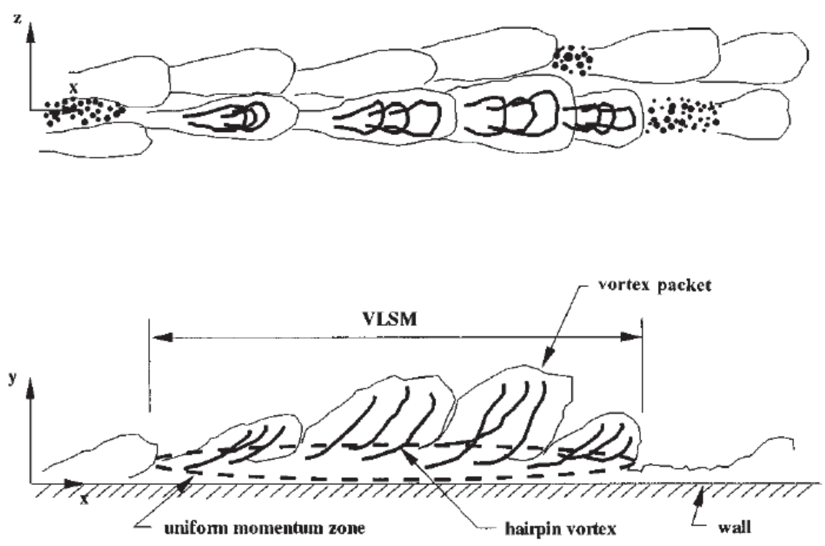

FIGURE 1.5: Conceptual model proposed by Kim and Adrian (1999) which describes the alignment of hairpins coherently into a package to form very large-scale motions.

Regarding to turbulence spectra aspects $k_x^{-5/3}$ and k_x^{-1} laws are widely discussed. Especially for characterizing the turbulence at high Reynolds numbers in wall-bounded flows these conditions are considered for the power spectral density of the streamwise fluctuating velocity component. According to these laws two overlapping cases of wavenumber ranges have been observed: overlap of the intermediate and high wavenumber ranges, the so-called $k_x^{-5/3}$ law, proposed by Kolmogorov (1941); and overlap of low and intermediate wavenumber ranges, the so-called k_x^{-1} law based on Perry and Abell (1977). Nickels et al. (2005) reported that the dependence based on k_x^{-1} can be observed at high Reynolds numbers while $k_x^{-5/3}$ law is a widely familiar condition in existing experiments. Vallikivi, Ganapathisubramani, and Smits (2015) concluded that the spectra collapses using both inner and outer scaling in pipe and boundary layer flows and k_x^{-1} region does not appear in all scalings, as well as in Zhao and Smits (2007). According to observation of Rosenberg et al. (2013) the overlap region and bi-modal distribution in energy spectrum vanishes with increasing Reynolds number. To estimate the locations of spectral peaks Rosenberg et al. (2013) developed a methodology where a Gaussian curve in $log(k_x)$ is fitted to data to determine the wavenumber peak location. Morrison et al. (2004), Rosenberg et al. (2013) and Vallikivi, Ganapathisubramani, and Smits (2015) also observed that no region exists where the spectra is collapsed using both scalings simultaneously. Additionally Morrison et al. (2004) suggested that u_τ may not be the correct velocity scale for obtaining a full overlap. Considering the spectra in Kolmogorov scaling in Vallikivi, Ganapathisubramani, and Smits (2015) the power law range with a slope close to $k_x^{-5/3}$ develops as wall-normal position increases, where the exponent is closer to -1.5 than $-5/3$.

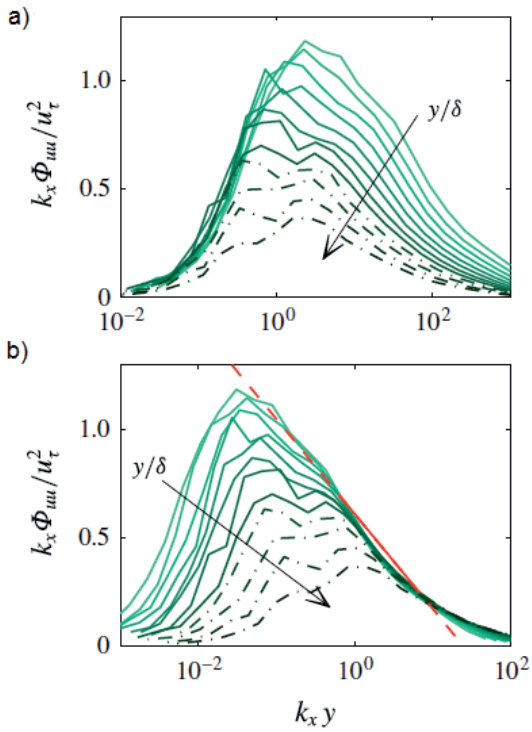

FIGURE 1.6: Premultiplied power spectra at $Re_\tau \approx 70.000$ with varying wall-normal locations in Superpipe scaled with R and wall distance respectively. Arrows indicate arrow indicates increasing y/R. (Vallikivi, Ganapathisubramani, and Smits (2015)) Red dashed lines proposed by Del Álamo et al. (2004).

It should also be noted that the flow behavior of various canonical geometries present different turbulence conditions regarding VLSMs. Balakumar and Adrian (2007) studied the same phenomena in the zero pressure gradient boundary layer and found out that with an increasing distance from the wall, the peak of the long wavelenght is decreasing in magnitude relative to the shorter wavelength which is the opposite case in channel flow. This gives an essential outline about bi-modal distribution of energy observing the power spectra. According to conclusion of Monty et al. (2009) the large-scale peak in energy spectra of internal flows appear at longer wavelengths than that in boundary layers. Same study draws an attention that VLSMs in internal flows should not be confused with superstructures (SS) in boundary layer flows, however these motions are similar but their energy in internal flows is stored at greater wall-normal distances and in larger wavelengths than the structures in boundary layer flows. Monty et al. (2009) also reported that the diversity between SS and VLSM may be occured by reason of different boundary conditions regarding to open and closed geometries. Furthermore Hutchins and Marusic (2007) observed that SS on flat plate are only present in the turbulent wall region while VLSM in pipe and channel are stretched to the outer flow. Considering the recent results of Vallikivi, Ganapathisubramani, and Smits (2015) on turbulence spectra in pipe and boundary layer, the outer flow in pipe can be still represented by LSMs and VLSMs which are associated with two major peaks in pre-multiplied power spectra, but in boundary layer flow only a single peak can be detected which leads to a sign of LSM. It can be concluded that the SS is not observable in the wake region at high Reynolds numbers.

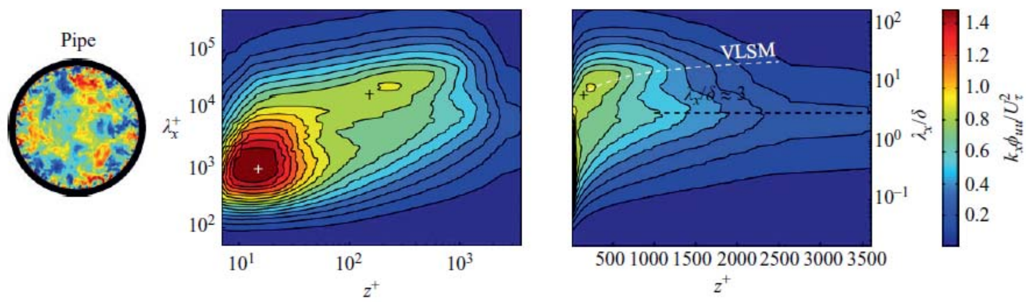

FIGURE 1.7: Contour maps of premultiplied spectra of streamwise velocity fluctuations in pipe flow as a function of outer and inner scaled wavelength and wall-normal location. (Monty et al. (2009))

1.3 Theoretical Background

Due to axisymmetry, pipe flow is one of the simplest geometries for investigating wall-bounded flows. In this section, theoretical background concerning turbulent pipe flow is presented, along a brief review of corresponding equations and fundamental explanations.

1.3.1 Pipe Flow Principals

For describing experimental results of pipe flow turbulence, a discussion on the fundamental equations is needed, which describes the phenomena in a mathematical way. Generally, Navier-Stokes equations for an incompressible flow written in Eulerian form as momentum balance can be used as first step, where the body forces are neglected (Equation 1.1):

$$\frac{\partial U}{\partial t} + (U \cdot \nabla)U = -\frac{1}{\rho}\nabla p + \nu \nabla^2 U \tag{1.1}$$

where U is the velocity vector, p is the pressure, ρ is the fluid density and ν is the kinematic viscosity, which can be determined as μ/ρ. On the other hand $\nabla \cdot U = 0$ describes the continuity equation for Newtonian and incompressible flows, which is already implemented in the above mentioned equation. Here the Reynolds decomposition technique can be applied to split the velocity parameter into its mean and fluctuating variables to indicate the streamwise velocity component (Equation 1.2):

$$U(x,t) = \overline{U}(x,t) + u(x,t) \tag{1.2}$$

where x stands for the streamwise direction, t for time, over-bar sign for averaged quantities and lower case parameter for fluctuations. Reynolds decomposition can be applied to the Navier-Stokes equations to determine the RANS - Reynolds averaged Navier-Stokes equations. In pipe flow, a cylindrical coordinate system (x, r, θ) should be defined to implement these equations to a circular boundary condition, where x indicates the axial, r the radial and θ the angular coordinate. In cartesian coordinate system, the velocity vector U can be written as (U, V, W), which describes streamwise, wall-normal and spanwise components respectively. Using the Reynolds decomposition, the mean variables are defined as $(\overline{U}, \overline{V}, \overline{W})$ and fluctuating variables as (u, v, w). Cartesian coordinate can be transformed to to cylindrical coordinates using Equation 1.3:

$$\nabla_{(x,r,\theta)} t = \begin{pmatrix} \frac{\partial t}{\partial x} \\ \frac{\partial t}{\partial r} \\ \frac{1}{x}\frac{\partial t}{\partial \theta} \end{pmatrix} \tag{1.3}$$

The resulting continuity equations can be written as following: